Metabolomics investigation of post-mortem human pericardial fluid

Alberto Chighine[1,2] · Matteo Stocchero[3] · Giulio Ferino[2] · Fabio De-Giorgio[4,5] · Celeste Conte[4,5] ·
Matteo Nioi[2] · Ernesto d'Aloja[2] · Emanuela Locci[2]

Abstract

Introduction Due to its peculiar anatomy and physiology, the pericardial fluid is a biological matrix of particular interest in the forensic field. Despite this, the available literature has mainly focused on post-mortem biochemistry and forensic toxicology, while to the best of authors' knowledge post-mortem metabolomics has never been applied. Similarly, estimation of the time since death or post-mortem interval based on pericardial fluids has still rarely been attempted.

Objectives We applied a metabolomic approach based on ^{1}H nuclear magnetic resonance spectroscopy to ascertain the feasibility of monitoring post-mortem metabolite changes on human pericardial fluids with the aim of building a multivariate regression model for post-mortem interval estimation.

Methods Pericardial fluid samples were collected in 24 consecutive judicial autopsies, in a time frame ranging from 16 to 170 h after death. The only exclusion criterion was the quantitative and/or qualitative alteration of the sample. Two different extraction protocols were applied for low molecular weight metabolites selection, namely ultrafiltration and liquid-liquid extraction. Our metabolomic approach was based on the use of ^{1}H nuclear magnetic resonance and multivariate statistical data analysis.

Results The pericardial fluid samples treated with the two experimental protocols did not show significant differences in the distribution of the metabolites detected. A post-mortem interval estimation model based on 18 pericardial fluid samples was validated with an independent set of 6 samples, giving a prediction error of 33–34 h depending on the experimental protocol used. By narrowing the window to post-mortem intervals below 100 h, the prediction power of the model was significantly improved with an error of 13–15 h depending on the extraction protocol. Choline, glycine, ethanolamine, and hypoxanthine were the most relevant metabolites in the prediction model.

Conclusion The present study, although preliminary, shows that PF samples collected from a real forensic scenario represent a biofluid of interest for post-mortem metabolomics, with particular regard to the estimation of the time since death.

Keywords Human pericardial fluid · ^{1}H NMR metabolomics · PMI · Extraction protocol · Time since death · Post-mortem

✉ Alberto Chighine
  alberto.chighine@unica.it

1 Cittadella Universitaria di Monserrato,
   09042 Monserrato (CA), Italy

2 Department of Medical Sciences and Public Health, Section
   of Legal Medicine, University of Cagliari, Cagliari, Italy

3 Department of Women's and Children's Health, University
   of Padova, Padova, Italy

4 Department of Health Care Surveillance and Bioethics,
   Section of Legal Medicine, Catholic University of Rome,
   Rome, Italy

5 Fondazione Policlinico Universitario A. Gemelli, IRCCS,
   Rome, Italy

Introduction

Pericardial fluid (PF) is a pale-yellow serous fluid present in the pericardial cavity, a virtual space that normally surrounds the heart with a volume, under physiological conditions, between approximately 15 and 60 mL. Historically it was believed that its physio-pathological role was limited to guarantee the cardiac cycle from the mechanical point of view, favoring the alternation of cardiac expansions and contractions. More recently, it has been demonstrated that PF production results not only on plasma ultrafiltration since its composition appears to be also sustained by secretion from pericardial mesothelial cells and myocardial interstitial space. Thus, this particular biofluid is supposed to carry

important information on the whole pericardial and cardiac homeostasis, with growing evidence indicating several bioactive molecules to be stored in the PF, suggesting a potential paracrine activity [1].

Scientific attention to PF has been limited by obvious and shareable ethical issues, as it is not possible to collect this biofluid from healthy donors, PF collections were always performed during open-heart surgery. In this setting, PF is certainly influenced by the pathological conditions affecting the surrounding structures (i.e., valvular, or ischemic cardiopathies), for which surgery is performed [2].

Recently, the attention of the scientific community has been devoted to PF chemical and biochemical composition [3-5], but little is known about the metabolic features of this particular biofluid. To our knowledge, only two papers can be found in literature dealing with PF lipidomics [6] and metabolomics [7]. The first was conducted on an animal model (rabbit) of hypercholesterolemia and coronary atherosclerosis, whereas the second investigated PF and plasma metabolome of patients undergoing cardiac surgery for coronary artery bypass grafting. Despite its use for forensic toxicological and biochemical purposes [8-12], post-mortem human PF has never been investigated with a metabolomic approach.

Our research group is focused on the application of metabolomics to address classical forensic issues by the analysis of different biological matrices on human and animal models [13], such as the identification of specific biofluids [14], the diagnosis of perinatal asphyxia [15, 16], the PMI estimation [17-20], the differential diagnosis of asphyxial deaths [21], and the diagnosis of drug-related fatalities [22]. Death is nowadays increasingly recognized as a dynamic rather than a static phenomenon [23], and we previously observed that multivariate approaches are more suitable than univariate to describe this multiparametric phenomenon. Time since death represents indeed the main driving force of post-mortem metabolome changes and we have previously highlighted the need for PMI standardization when post-mortem metabolomics is performed for aims different than PMI [24].

PMI estimation still represents one of the biggest forensic conundrums, with a large body of forensic literature aiming at the discovery of accurate and reliable tools for its determination, sadly often far away from practical application [25]. The ideal biofluid to be studied in metabolomics for PMI estimation should be relatively stable to display monitorable time-related metabolome modifications. Such characteristics are usually found in ocular biofluids due to the unique anatomical and physiological features [26, 27]. Like ocular biofluids, PF appears suitable for post-mortem investigations as its confined anatomy and physiology may offer a relative resistance to post-mortem autolysis and putrefaction. Furthermore, this biofluid has shown remarkable stability in an animal model, with a slow turnover rate ranging between 5.4 and 7.2 h [27-29]. To date, only one investigation aimed at estimating PMI on human PF was performed and was based on changes in electrolyte concentration over a time window of 2.5–85.0 h [30]. Another study, performed on an animal model (rabbit), investigated shorter PMIs (up to 48 h) based on Fourier transform infrared spectroscopy and chemometrics [31].

To the best of our knowledge, this is the first study dealing with post-mortem human PF metabolomics. The objective of this proof-of-concept study was to investigate the feasibility of PF metabolomics to estimate PMI. To this aim, PF samples collected during 24 consecutive judicial autopsies were analyzed with ^{1}H Nuclear Magnetic Resonance (NMR) spectroscopy following two different experimental protocols for the analysis of the metabolome.

Materials and methods

Sample collection

PF samples were collected during 24 consecutive judicial autopsies performed at Forensic and Legal Medicine Institute of University of Cagliari. After routine opening of the chest wall, pericardium was anteriorly dissected through a reversal 'Y' incision which allowed pericardial cavity to be exposed. The cardiac apex was gently pulled up and declivous PF was collected with a sterile no-needled syringe. Collection was not performed in case of pathological pericardial effusion and/or macroscopic blood contamination. Not all the PMIs were precisely known, being estimated based on circumstantial evidence and/or classical thanatological signs. After collection, PFs were immediately stored at − 80 °C.

Sample preparation for NMR analysis

Before NMR analysis, samples were thawed, centrifuged for 10 min at 13000 g and 4 °C and the supernatant was divided in two aliquots, that were treated in two different ways for protein removal. An aliquot of 500 µl was submitted to ultrafiltration (U) while the second was extracted using a liquid-liquid extraction (LLE) procedure. Ultrafiltration was performed using 10 kDa filter units (Amicon-10 kDa; Merck Millipore, Darmstadt, Germany) for 25 min at 13,000 g and 4 °C. Filters were previously washed out from glycerol by adding 500 µl of distilled water and by centrifuging for 5 min at 13,000 g at room temperature for 15 times. For the NMR analysis, 300 µl of filtered PF were diluted with 400 µl of a 0.09-M phosphate buffer solution (pH = 7.4) in D_2O (99,9%, Cambridge Isotope Laboratories Inc., Andover, USA) containing the internal

standard sodium 3 (trimethylsilyl)propionate-2,2,3,3,-d_4 (TSP, 98 atom % D, Sigma-Aldrich, Milan) at a 0.21 mM final concentration, and 650 µl of the final solution were transferred into a 5 mm NMR tube. For LLE, an aliquot of 400 µl was mixed with 1200 µl of a chloroform: methanol (1:1, both HPLC grade, Honeywell, Germany) solution and 175 µl of Milli-Q water. The samples were vortexed and centrifuged at 1700 g for 30 min at room temperature. The upper hydrophilic phase was dried overnight using a speed vacuum centrifuge (Eppendorf concentrator plus, Eppendorf AG, Hamburg, Germany). The dried samples were rehydrated by adding 300 µl of D_2O and 400 µl of a 0.09-M phosphate buffer solution (pH = 7.4) in D_2O containing TSP at a 0.21 mM final concentration. Six hundred fifty microliters of the resulting solution were transferred into a 5-mm NMR tube. One PF sample was analyzed without any pre-treatment. After thawing and centrifugation, 300 µl of PF were diluted with 400 µl of the phosphate buffer solution previously used, and 650 µl of the final solution were transferred into a 5-mm NMR tube.

^{1}H NMR experiments and data processing

^{1}H NMR experiments were carried out on a Varian UNITY INOVA 500 spectrometer (Agilent Technologies, CA, USA) operating at 499.839 MHz. Spectra were acquired at 300 K using a spectral width of 6000 Hz, a 90° pulse, an acquisition time of 1.5 s, a relaxation delay of 2 s, and 256 scans. Non treated PF and UPF spectra were acquired using the standard 1D NOESY pulse sequence for water suppression with a mixing time of 1 ms and a recycle time of 21.5 s, while in LLEPF spectra the residual water signal was suppressed by applying a standard presat pulse sequence with low-power radiofrequency irradiation for 2 s during relaxation. Spectra were processed using MestReNova software (Version 9.0, Mestrelab Research S.L.). The free induction decays (FID) were multiplied by an exponential weighting function equivalent to a line broadening of 0.5 Hz and zero-filled to 128 K before Fourier transformation. All spectra were phased, baseline corrected, and referenced to TSP at 0.00 ppm. The assignment of the metabolites in the ^{1}H NMR spectra was performed based HMDB database (http://www.hmdb.ca), Chenomx NMR Suite 8.2 Library (Chenomx Inc., Edmonton, Canada), and comparison with spectra of standard compounds recorded using the same experimental conditions. Moreover, using the Chenomx NMR Suite Profiler tool a set of 50 quantified metabolites was obtained, after the exclusion of exogenous metabolites such as ethanol, caffeine and drugs (see Supplementary Table S1). The final data set was exported as a text file for multivariate statistical data analysis. Data were autoscaled prior to performing data analysis.

Multivariate statistical data analysis

Exploratory data analysis was performed by Principal Component Analysis (PCA) [32] to discover outliers and specific trends in the data. Regression models to estimate PMI from the quantified metabolites were based on orthogonally Constrained PLS2 (oCPLS2) [33]. The application of orthogonal constraints to PLS-regression was necessary to avoid that the factor age affected the models. Indeed, oCPLS2 guaranteed score components orthogonal to age, modeling data variation mainly associated to PMI. Relevant predictors were discovered by stability selection using the Variable Influence on Projection (VIP) score in variable selection [34]. Specifically, 200 subsamples were extracted by Binary Matrix Sampling with probability 0.7. For each subsample, the subset of predictors that generated the oCPLS2 model with the best performance in cross-validation was calculated. The frequency of selection of each predictor was compared with that of a random choice to discover the relevant predicators. A significance level of 0.05 was assumed. Repeated 5-fold cross-validation with 20 repetitions was applied in model optimization maximizing the R^2 on the validation set, i.e., Q^2. Randomization test was applied to discover over-fitting and to assess the reliability of the model. The data variation of the relevant metabolites discovered by PLS-based analysis was investigated by Multiple Linear Regression (MLR) considering the factors age and PMI. A stratified random selection procedure based on the different ranges of PMI was applied to select a training set for model building and a test set for model validation. PCA was performed by Simca 14 (Umetrics, Sweden), whereas oCPLS2 and MLR-based analysis were implemented by in-house R-functions developed using R 4.0.4 (R Foundation for Statistical Computing, Vienna).

Results

PF were collected from corpses of both gender (with a M to F ratio of approximately 1:3), aged from 20 to 87 years (mean = 51, SD = 21) with a PMI ranging from 16 to 170 h (mean = 70, SD = 46). Table 1 reports the demographic data, PMI, and causes of death. It is worth noting that PMI and age showed a moderate correlation ($r = 0.35$, $p = 0.09$), whereas no significant association was discovered for PMI and sex. A training set composed of 18 samples and a test set of 6 samples were selected. The distributions of sex and age in the training set were the same observed in the collected samples.

Before NMR analysis, PF samples were treated in two different ways, namely ultrafiltration and liquid-liquid extraction, in view of the possibility of the future use of other analytical platforms based on mass spectrometry (MS) besides

Table 1 Demographic parameters, PMI and causes of death

Sample	Sex	Age	PMI (h)	Cause of death
1	F	31	16	Haemorrhagic shock
2	M	20	20	Mechanical asphyxia (hanging)
3	M	35	25	Acute cardiac failure
4	M	21	32	Epidural hematoma
5	M	87	33	Subdural hematoma
6	F	52	33.5	Cardiogenic shock (myocardial infarction)
7	M	68	38	Haemorrhagic/traumatic shock
8	M	63	39	Mechanical asphyxia (positional)
9	F	81	41	Acute cardiac failure
10	M	32	46	Drug intoxication (cocaine)
11	M	38	46	Mechanical asphyxia (hanging)
12	F	60	62	Pulmonary embolism and cerebellar ischemia
13	M	42	63	Cerebral ischemia
14	M	37	66	Haemorrhagic shock
15	M	49	70.3	Mechanical asphyxia (*ab ingestis*)
16	F	39	77	Multiorgan failure
17	M	28	82	Drug intoxication (cocaine, heroin)
18	M	58	86	Acute bowel infarction
19	M	32	92	Hypoxic brain death
20	M	81	100	Haemorrhagic shock
21	F	77	120	Neoplastic cachexia
22	M	42	160	Drug intoxication (buprenorphine)
23	F	69	168	Neoplastic cachexia
24	M	80	170	Acute cardiac failure

NMR. Indeed, MS techniques would allow us to expand the explorable metabolome of PF samples to other classes of molecules such as the more lipophilic ones. While NMR does not need strong manipulation of the biofluids, requiring only the elimination of large molecules such as proteins or lipids, MS techniques are mainly based on more invasive liquid-liquid extraction procedures with appropriate solvents. In this view, it is important to ensure that the extraction protocol does not significantly affect either qualitatively or quantitatively the metabolome. To this aim, we compared the spectra of ultrafiltered PF (UPF) with the spectra of the hydrophilic phase of the liquid-liquid extracted PF (LLEPF). We also recorded a spectrum of an untreated PF samples.

Figure 1 shows the aliphatic part of the ^{1}H NMR spectrum of the untreated PF compared to the spectra of UPF and LLEPF. It is worth of note that the three samples were taken from the same individual, in order to compare the different experimental treatment without having to consider the interindividual variability. As can be seen, untreated PF (Fig. 1A) exhibits broad resonances from macromolecules causing baseline distortion and interfering with the sharp resonances originating from low molecular weight metabolites. After removal of the macromolecules, both UPF (Fig. 1B) and LLEPF (Fig. 1C) give spectra with proper baselines showing only the required

sharp resonances from small metabolites. Interestingly, the two NMR spectra of the protein-free samples are extremely similar. The main difference between them is the absence of ethanol in the LLEPF spectrum, as can be expected due to the sample concentration step required in the LLE procedure.

Twenty-four PF samples collected during consecutive autopsies from cadavers with PMI ranging from 16 to 170 h were then processed using both experimental protocols. A total of 48 PF were analyzed by ^{1}H NMR. Comparison of all the 48 spectra recorded following the two experimental protocol, shows the absence of any significant qualitative or quantitative difference in the distribution of the recorded NMR resonances assigned to the small metabolites, indicating that proteins and/or other large molecules are equally excluded both with the physical procedure of filtering and with solvent extraction (Supplementary Fig. S1). Fifty identified metabolites were quantified in both the datasets using the Chenomx NMR Suite Profiler tool (see Supplementary Table S1). The matrix of the quantified metabolites was submitted to multivariate analysis. Principal Component Analysis (PCA) was first applied to investigate trends and similarities among the spectra (Fig. 2). No outliers were detected by T2 and Q-distance test assuming a significance level of 0.05 considering each single data set.

Fig. 1 Aliphatic part of the ^{1}H NMR spectrum of untreated PF (**A**), UPF (**B**), and LLEPF (**C**) samples. Three PF aliquots of the same individual were analyzed. (*) indicates the triplet of ethanol
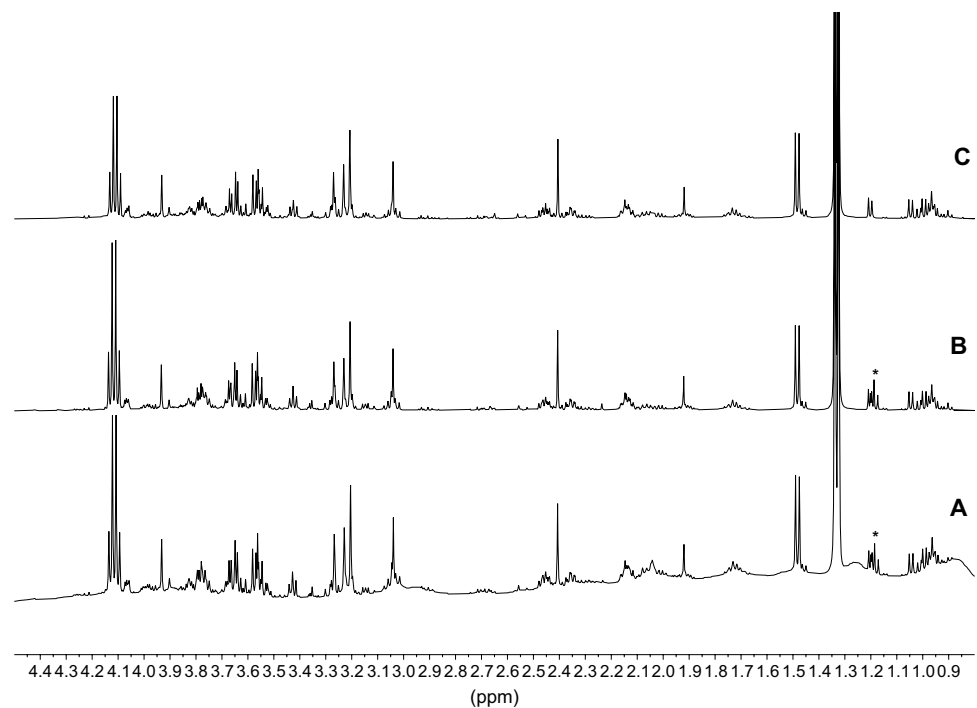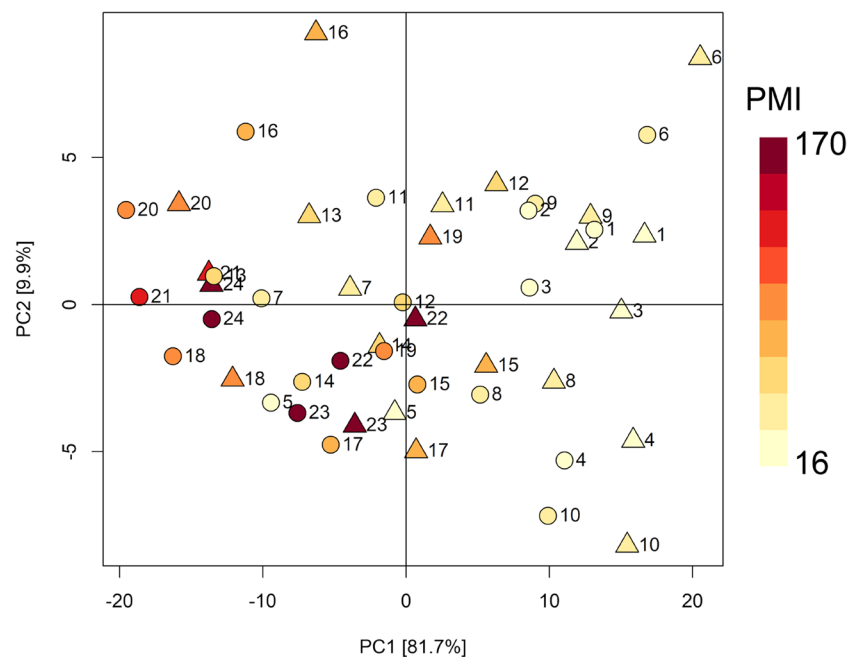

Fig. 2 PCA model of PF samples. Samples are colored by PMI (range has been divided in 9 equally spaced intervals) and labeled according to individual. Different symbols represent the extraction method (U: triangles; LLE: circles)

As can be seen in Fig. 2, the two PF samples belonging to the same individual are very similar, lying in the same region of the multivariate space of the first two PCs, independently of the pre-analytical processing used. The observed scattering between the two samples of the same individuals reflects the sum of the experimental errors coming from the extraction, the instrumental precision, the post-processing and fitting of the spectra, but it does not affect the global distribution of the samples and therefore the global metabolomic features. Of note, a time-related trajectory can be observed along PC1.

Supervised data analysis based on projection to latent structure regression (PLS) was applied to evaluate the effects of PMI on the metabolomic profiles of the collected PF samples. Considering the data set obtained from UPF samples, the oCPLS2 model showed 1 predictive score component, $R^2 = 0.547$ ($p = 0.045$), $Q^2 = 0.244$ ($p = 0.010$), standard deviation error in calculation (SDEC) equal to 30 h, mean
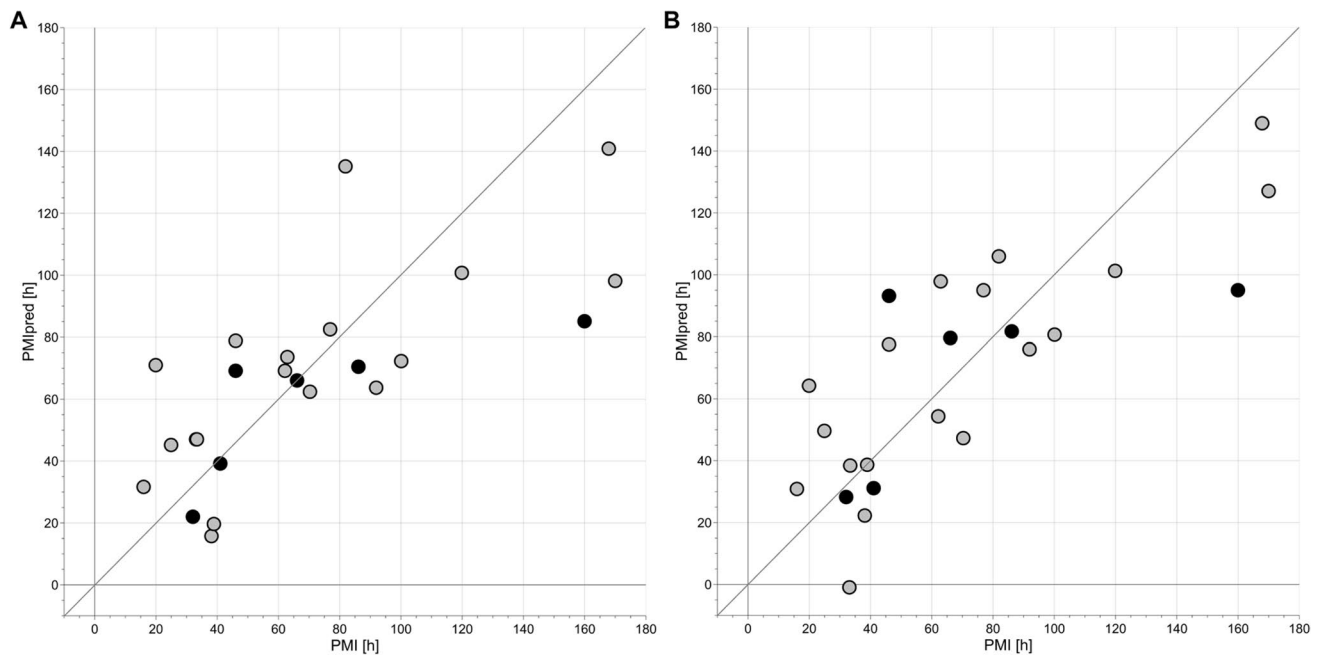
Fig. 3 PMI calculated for the training set (grey circles) and predicted for the test set (black circles) vs experimental PMI for PMI in the range [16, 170] h. **A** reports the results for the data obtained from UPF samples, while **B** those from LLEPF

standard deviation error in cross-validation (SDECV) equal to 38 h and standard deviation error in prediction (SDEP) equal to 33 h. In Fig. 3A, the PMI calculated for the training set and that predicted for the test set are reported. It is worth noting that samples with the highest PMI showed the worst estimate of PMI, with a negative deviation with respect to

the experimental value. This may be due to a change of the biological mechanisms determining the metabolic content of PF at the highest PMI that may introduce a mild non-linearity in the behavior of the metabolic concentration with respect to PMI. Unfortunately, the interval between 120 and 160 h was not sampled and therefore it is not possible to investigate
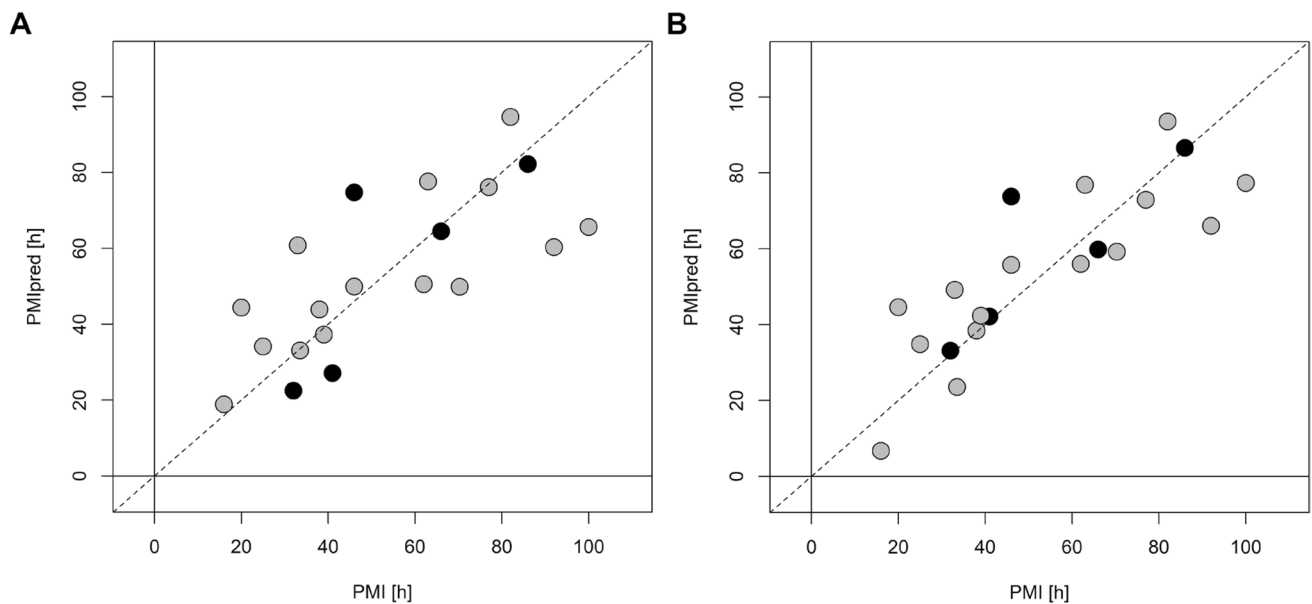

Fig. 4 PMI calculated for the training set (grey circles) and predicted for the test set (black circles) vs experimental PMI for PMI in the range [16, 100] h. **A** reports the results for the data obtained from UPF samples, while **B** those from LLEPF

Table 2 Relevant metabolites discovered by oCPLS2 analysis

Metabolite	Protocol	r	p
Acetate	LLE	0.387	0.169
	U	0.403	0.150
Betaine	LLE	0.199	0.495
	U	0.317	0.267
Butyrate	U	0.641	**0.012**
Choline	LLE	0.539	**0.043**
	U	0.606	**0.019**
Citrate	LLE	-0.605	**0.019**
Ethanolamine	LLE	0.633	**0.013**
	U	0.632	**0.013**
Formate	LLE	0.554	**0.037**
	U	0.556	**0.036**
Glycine	LLE	0.728	**0.002**
	U	0.723	**0.003**
Hypoxanthine	LLE	-0.630	**0.014**
	U	-0.559	**0.035**
Inosine	LLE	-0.419	0.132
	U	-0.358	0.206
Mannose	LLE	-0.436	0.115
Methanol	LLE	-0.461	0.093
	U	-0.267	0.355
Myo-inositol	U	-0.036	0.902
Nicotinurate	LLE	0.255	0.377
Proline	U	0.641	**0.011**
Propionate	U	0.536	**0.045**
β-Alanine	U	0.279	0.333
Trimethylamine	LLE	0.508	**0.060**
	U	0.561	**0.034**
Uracil	U	0.700	**0.004**
Uridine	U	0.266	0.357

Protocol specifies the type of experimental protocol applied for protein removal, r is the Pearson's correlation coefficient between metabolite concentration corrected by age and PMI, and p is the p value of the coefficient of PMI in the MLR regression model that uses PMI and age as factors and metabolite concentration as response

Bold values indicate a significance level <0.05

more in detail the behavior of PMI in that interval, where non-linearity seems to appear. If PMI greater than 100 h are not considered in the analysis, a oCPLS2 model with 1 predictive score component, $R^2 = 0.543$ ($p = 0.030$), $Q^2 = 0.444$ ($p = 0.005$), SDEC = 17 h, SDECV = 19 h and SDEP = 15 h, can be obtained. As it can be observed in Fig. 4A, where PMI calculated for the training set and that predicted for the test set

are reported, the behavior of PMI estimated by the model, i.e., the predictive score component, shows a linear behavior with respect to the experimental PMI. Stability selection applied to the model built considering the whole range of PMI discovered 17 metabolites as significantly relevant, 10 of which resulted to be significantly related to PMI after correction by age (Table 2). The data set obtained from LLEPF samples led
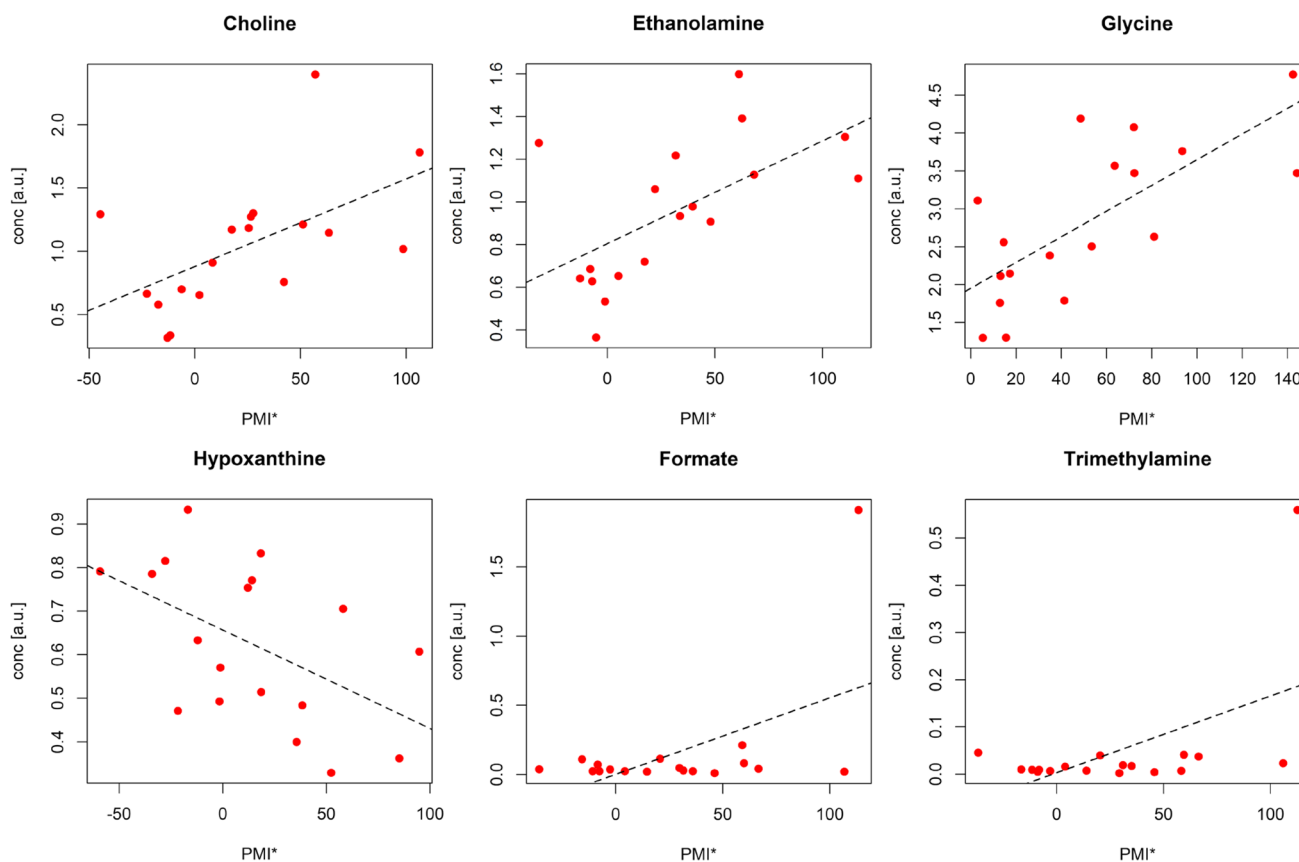
Fig. 5 Data obtained from UPF dataset: profiles of the metabolite concentration corrected by age (conc*) vs PMI for the relevant metabolites discovered using datasets from both UPF and LLEPF. Only metabolites with p less than 0.10 are reported

to a regression model with 1 predictive and 1 non-predictive score component, $R^2 = 0.669$ ($p = 0.065$), $Q^2 = 0.161$ ($p = 0.045$), SDEC = 25 h, SDECV = 41 h, and SDEP = 34 h. In Fig. 3B, the PMI calculated for the training set and that predicted for the test set are reported. Also in this case, a mild non-linearity is observed in the data. If PMI greater than 100 h are not considered, a oCPLS2 model with 1 predictive score component, $R^2 = 0.701$ ($p = 0.005$), $Q^2 = 0.569$ ($p = 0.005$), SDEC = 14 h, SDECV = 17 h and SDEP = 13 h, can be obtained. The PMI calculated for the training set and that predicted for the test set are reported in Fig. 4B. As in the case of the data set obtained by ultrafiltration, the behavior of PMI estimated by the model shows a linear behavior with respect to the experimental PMI. Applying stability selection to the model built considering the whole data set, 13 metabolites resulted to be relevant, 7 of which resulted to be significantly related to PMI (Table 2).

The profiles of the relevant metabolites mainly related to PMI common to both data sets are reported in Fig. 5 (data from UPF samples are shown). Similar profiles were observed for the data obtained from LLEPF samples (data not shown). Interestingly, formate and trimethylamine show a sudden increase at the highest PMI. The same trend is observed for propionate in UPF samples. This may be due to the presence of outliers or to a real change in the biological mechanism underlying PMI. Further investigations are requested to investigate more in depth this finding. When the reduced PMI range (16–100 h) is considered, the relevant metabolites related to PMI do not change except for formate and trimethylamine that are not significant anymore, further corroborating the hypothesis that they are only related to higher PMIs.

Discussion

Considering that little is known about the PF metabolomic composition, our first objective was to establish whether the analytical protocol used to extract the metabolites could influence the detectable metabolome. PCA analysis clearly shows that the distribution of PF samples is maintained regardless of the protocol used, indicating that the explored metabolome remains unaffected. In our previous works, we investigated post-mortem metabolomics through ^{1}H NMR analysis of biofluids processed via ultrafiltration [17, 18, 20, 21]. However, in the perspective of using multiple analytical platforms, expanding toward mass spectrometry, we

explored the use of two different experimental protocols. The main difference we observed is that LLE allows to rule out ethanol, typically present in high concentrations in real-life forensic samples, the NMR resonances of which is overlapped to signals of endogenous molecules of interest (among all 3-hydroxybutyrate).

Furthermore, since sampling was essentially performed with no exclusion criteria, except for obvious PF pathological appearance, the metabolomic composition did not appear related to sex and cause of death, although a moderate correlation was observed between PMI and age.

Post-mortem modifications in the PF metabolome were found to be correlated with PMI, so that a predictive model for PMI estimation was built and rigorously validated with an independent test set of PF samples. The error in prediction was very similar in the two experimental datasets (33 and 34 h for U and LLE, respectively) over the studied PMI window (16–170 h). Samples with PMI greater than 100 h were characterized by the highest errors in prediction, suggesting an underlying biological mechanism which could result in a non-linear behavior. This is somehow expectable as bacterial growth occurs at later PMIs, resulting in a co-metabolism. We have previously observed this phenomenon in a highly controlled animal model of PMI estimation on aqueous and vitreous humor samples [17, 18, 20]. Since in the present experiment the interval between 120 and 160 h, when non-linearity seems to appear, was not adequately sampled, it was not possible to better investigate the behaviour of the metabolome in this interval. Interestingly, some of the longer PMI samples display however several features proper of bacterial metabolism, namely formate, trimethylamine, propionate and butyrate.

Due to the aforementioned, we have decided to focus on the more homogeneously covered PMI window, i.e., up to 100 h. This strategy led to a remarkable improvement of the prediction model in both experimental protocols with errors in prediction of 15 and 13 h, for U and LLE, respectively.

The design of the experiment was certainly underpowered to make any conclusive inferences about the underlying metabolic phenomena. Despite this, 20 metabolites were relevant in the PMI regression, 11 out of 20 were shared by U and LLE protocols. Among the latter, choline, ethanolamine, glycine, hypoxanthine, formate, and trimethylamine were statistically significant ($p < 0.10$) with respect to PMI. Taking into consideration PMI up to 100 h, formate and trimethylamine were no more significant, confirming their role only in very late PMI. Of note, among the 4 remaining metabolites, hypoxanthine was the only one with a decreasing behaviour, whereas choline, ethanolamine and glycine were directly related to PMI. Intriguingly, the very same 4 metabolites appeared to be correlated with PMI on our recent estimation model built on sheep's VH in a similar time-window, suggesting a

shared post-mortem metabolome derangement despite the different biological matrix and species under investigation [20]. Furthermore, such finding is consistent with literature as choline [17, 18, 35–37], hypoxanthine [19, 38–40], glycine [35], and formate [39] have been demonstrated to be related with PMI in different biological matrices in both animal and human models.

Mizutani et al. observed stable 3-hydroxybutyrate levels in post-mortem human PF within 96 h after death [12]. Interestingly, this trend was also observed in our data, even in samples with higher PMIs (up to 170 h), confirming this metabolite's resilience to post-mortem in human PF.

Our study has several limitations. Firstly, due to its proof-of-concept nature, only a limited number of samples were analyzed. Secondly, random sampling did not allow to homogeneously cover the entire time-window investigated, with an underrepresentation of PMI > 100 h. Thirdly, PFs were taken from consecutive judicial cases and in many of them the PMI was estimated through circumstantial evidence and/or classical thanatological signs; most of the corpses were stored cooled in the morgue before autopsy for an uneven time. Finally, the samples were analyzed through a single analytical platform which is not appropriate for investigating the lipophilic phase.

Despite these limitations, the presented results show that the spectrum of biological activity associated with post-mortem modifications in a real-life scenario can be intercepted by the proposed approach, independently of a number of major variables, namely cause and mechanism of death, sex, and corpse storage. Additionally, notwithstanding the limited sampling, PMI was accurately predicted using an independent set of samples with error as low as 13 h for PMI ≤ 100 h. Moreover, we demonstrated that the metabolite extraction procedure did not alter the metabolome composition and can therefore be independently selected according to the chosen analytical platform.

Conclusions

In conclusion, PF was found to be a biofluid of interest for post-mortem metabolomics. Hence, this proof-of-concept approach deserves to be translated on a wide dataset and investigated with different analytical platforms. Due to the peculiar physiopathology, PF metabolomics appears intriguing to investigate the cause and mechanism of death, unless modifications related to PMI are fully taken into account, either standardizing the samples according to PMI or constraining the model to this factor.

Declarations

References

1. Trindade F, Vitorino R, Leite-Moreira A, Falcão-Pires I (2019) Pericardial fluid: an underrated molecular library of heart conditions and a potential vehicle for cardiac therapy. Basic Res Cardiol 114:10. https://doi.org/10.1007/s00395-019-0716-3

2. Fatehi Hassanabad A, Zarzycki A, Deniset JF, Fedak PW (2021) An overview of human pericardial space and pericardial fluid. Cardiovasc Pathol 53:107346. https://doi.org/10.1016/j.carpath.2021.107346

3. Buoro S, Tombetti E, Ceriotti F, Simon C, Cugola D, Seghezzi M, Innocente F, Maestroni S, Del Carmen Baigorria Vaca M, Moioli V, Previtali G, Manenti B, Adler Y, Imazio M, Brucato A (2021) What is the normal composition of pericardial fluid? Heart 107:1584–1590. https://doi.org/10.1136/heartjnl-2020-317966

4. Imazio M, Biondo A, Ricci D, Boffini M, Pivetta E, Brucato A, Giustetto C, De Ferrari GM, Rinaldi M (2020) Contemporary biochemical analysis of normal pericardial fluid. Heart 106:541–544. https://doi.org/10.1136/heartjnl-2018-314574

5. Ben-Horin S, Shinfeld A, Kachel E, Chetrit A, Livneh A (2005) The composition of normal pericardial fluid and its implications for diagnosing pericardial effusions. Am J Med 118:636–640. https://doi.org/10.1016/j.amjmed.2005.01.066

6. Tamura S, Koike Y, Takeda H, Koike T, Izumi Y, Nagasaka R, Tsunoda T, Tori M, Ogawa K, Bamba T, Shiomi M (2018) Ameliorating effects of D-47, a newly developed compound, on lipid metabolism in an animal model of familial hypercholesterolemia (WHHLMI rabbits). Eur J Pharmacol 822:147–153. https://doi.org/10.1016/j.ejphar.2018.01.013

7. Yang Y, Du Z, Fang M, Ma Y, Liu Y, Wang T, Han Z, Peng Z, Pan Y, Qin H, Qin Y, Jiang Y, Tu P, Guo X, Lu Y, Yang X, Hua K (2023) Metabolic signatures in pericardial fluid and serum are associated with new-onset atrial fibrillation after isolated coronary artery bypass grafting. Transl Res 256:30–40. https://doi.org/10.1016/j.trsl.2023.01.001

8. Cabarcos-Fernández P, Tabernero-Duque MJ, Álvarez-Freire I, Bermejo-Barrera AM (2021) Determination of seven antidepressants in pericardial fluid by means of dispersive liquid-liquid microextraction (DLLME) and gas chromatography-mass spectrometry (GC/MS). J Anal Toxic 46:146–156. https://doi.org/10.1093/jat/bkab003

9. Ferreira E, Corte Real F, Melo Pinho E, T, Margalho C, (2020) A Novel Bioanalytical Method for the Determination of Opioids in Blood and Pericardial Fluid. J Anal Toxic 44:754–768. https://doi.org/10.1093/jat/bkaa064

10. Tominaga M, Michiue T, Ishikawa T, Inamori-Kawamoto O, Oritani S, Maeda H (2015) Evaluation of postmortem drug concentrations in cerebrospinal fluid compared with blood and pericardial fluid. For Sci Int 254:118–125. https://doi.org/10.1016/j.forsciint.2015.07.005

11. Takasu S, Matsumoto S, Kodama S, Sakamoto K, Shimmura S, Iwadate K (2022) Accuracy of urea nitrogen and creatinine measurements in postmortem serum and pericardial fluid compared with antemortem data. Am J Forensic Med Pathol 43:33–39. https://doi.org/10.1097/PAF.0000000000000710

12. Mizutani T, Yoshimoto T, Ishii A (2018) Pericardial fluid is suitable as an alternative specimen for the measurement of β-hydroxybutyrate within 96 h after death. Legal Med (Tokyo) 33:53–54. https://doi.org/10.1016/j.legalmed.2018.05.004

13. Locci E, Bazzano G, Chighine A, Locco F, Ferraro E, Demontis R, d'Aloja E (2020) Forensic NMR metabolomics: one more arrow in the quiver. Metabolomics 16:118. https://doi.org/10.1007/s11306-020-01743-6

14. Scano P, Locci E, Noto A, Navarra G, Murgia F, Lussu M, Barberini L, Atzori L, De Giorgio F, Rosa MF, d'Aloja E (2013) ¹H NMR metabolite fingerprinting as a new tool for body fluid identification in forensic science. Magnetic Reson Chem 51:454–462. https://doi.org/10.1002/mrc.3966

15. Locci E, Noto A, Puddu M, Pomero G, Demontis R, Dalmazzo C, Delogu A, Fanos V, d'Aloja E, Gancia P (2018) A longitudinal ¹H-NMR metabolomics analysis of urine from newborns with hypoxic-ischemic encephalopathy undergoing hypothermia therapy. Clinical and medical legal insights. PloS One 13:e0194267. https://doi.org/10.1371/journal.pone.0194267

16. Locci E, Bazzano G, Demontis R, Chighine A, Fanos V, d'Aloja E (2020) Exploring Perinatal Asphyxia by Metabolomics. Metabolites 10:141. https://doi.org/10.3390/metabo10040141

17. Locci E, Stocchero M, Noto A, Chighine A, Natali L, Napoli PE, Caria R, De-Giorgio F, Nioi M, d'Aloja E (2019) A ¹H NMR metabolomic approach for the estimation of the time since death using aqueous humour: an animal model. Metabolomics 15:76. https://doi.org/10.1007/s00414-023-02975-6

18. Locci E, Stocchero M, Gottardo R, De-Giorgio F, Demontis R, Nioi M, Chighine A, Tagliaro F, d'Aloja E (2021) Comparative use of aqueous humour ¹H NMR metabolomics and potassium concentration for PMI estimation in an animal model. Int J Leg Med 135:845–852. https://doi.org/10.1007/s00414-023-02975-6

19. Bonicelli A, Mickleburgh HL, Chighine A, Locci E, Wescott DJ, Procopio N (2022) The 'ForensOMICS' approach for postmortem interval estimation from human bone by integrating metabolomics, lipidomics, and proteomics. eLife 11:e83658. https://doi.org/10.7554/eLife.83658

20. Locci E, Stocchero M, Gottardo R, Chighine A, De-Giorgio F, Ferino G, Nioi M, Demontis R, Tagliaro F, d'Aloja E (2023) PMI estimation through metabolomics and potassium analysis on animal vitreous humour. Int J Legal Med. https://doi.org/10.1007/s00414-023-02975-6

21. Locci E, Chighine A, Noto A, Ferino G, Baldi A, Varvarousis D, Xanthos T, De-Giorgio F, Stocchero M, d'Aloja E (2021) Metabolomics improves the histopathological diagnosis of asphyxial deaths: an animal proof-of-concept model. Sci Rep 11:10102. https://doi.org/10.1038/s41598-021-89570-0

22. Chighine A, Porcu M, Ferino G, Lenigno N, Trignano C, d'Aloja E, Locci E (2022) Infant urinary metabolomic profile in a fatal acute methadone intoxication. Int J Leg Med 136:569–575. https://doi.org/10.1007/s00414-021-02772-z

23. Ferreira PG, Muñoz-Aguirre M, Reverter F, Sá Godinho CP, Sousa A, Amadoz A, Sodaei R, Hidalgo MR, Pervouchine D, Carbonell-Caballero J, Nurtdinov R, Breschi A, Amador R, Oliveira P, Çubuk C, Curado J, Aguet F, Oliveira C, Dopazo J et al (2018) The effects of death and post-mortem cold ischemia on human tissue transcriptomes. Nat Commun 9:490. https://doi.org/10.1038/s41467-017-02772-x

24. Chighine A, Locci E, Nioi M, d'Aloja E (2021) Looking for post-mortem metabolomic standardization: waiting for godot-the importance of post-mortem interval in forensic metabolomics. Chemical Res Toxicol 34:1946–1947. https://doi.org/10.1021/acs.chemrestox.1c00211

25. Gelderman T, Stigter E, Krap T, Amendt J, Duijst W (2021) The time of death in Dutch court; using the Daubert criteria to evaluate methods to estimate the PMI used in court. Leg Med (Tokyo) 53:101970. https://doi.org/10.1016/j.legalmed.2021.101970

26. Ang JL, Collis S, Dhillon B, Cackett P (2021) The Eye in Forensic Medicine: A Narrative Review. Asia Pac J Ophthalmol (Philadelphia) 10:486–494. https://doi.org/10.1097/APO.0000000000000426

27. Pigaiani N, Bertaso A, De Palo EF, Bortolotti F, Tagliaro F (2020) Vitreous humor endogenous compounds analysis for post-mortem forensic investigation. Forensic Sci Int 310:210235. https://doi.org/10.1016/j.forsciint.2020.110235

28. Boulanger B, Yuan Z, Flessner M, Hay J, Johnston M (1999) Pericardial fluid absorption into lymphatic vessels in sheep. Microvascular Res 57:174–186. https://doi.org/10.1006/mvre.1998.2127

29. Vogiatzidis K, Zarogiannis SG, Aidonidis I, Solenov EI, Molyvdas PA, Gourgoulianis KI, Hatzoglou C (2015) Physiology of pericardial fluid production and drainage. Front Physiol 6:62. https://doi.org/10.3389/fphys.2015.00062

30. Singh D, Prashad R, Sharma SK, Pandey AN (2006) Estimation of postmortem interval from human pericardial fluid electrolytes concentrations in Chandigarh zone of India: log transformed linear regression model. Leg Med (Tokyo) 8:279–287. https://doi.org/10.1016/j.legalmed.2006.06.004

31. Zhang J, Li B, Wang Q, Wei X, Feng W, Chen Y, Huang P, Wang Z (2017) Application of Fourier transform infrared spectroscopy with chemometrics on postmortem interval estimation based on pericardial fluids. Sci Rep 7:18013. https://doi.org/10.1038/s41598-017-18228-7

32. Jolliffe IT (1986) Principal component analysis. Springer Series in Statistics. Springer, New York, NY. https://doi.org/10.1007/978-1-4757-1904-8

33. Stocchero M, Riccadonna S, Franceschi P (2018) Projection to latent structures with orthogonal constraints for metabolomics data. J Chemometr 32:e2987. https://doi.org/10.1002/cem.2987

34. Stocchero M (2020) Relevant and irrelevant predictors in PLS2. J Chemometr 34:e3237. https://doi.org/10.1002/cem.3237

35. Zelentsova EA, Yanshole LV, Melnikov AD, Kudryavtsev IS, Novoselov VP, Tsentalovich YP (2020) Post-mortem changes in metabolomic profiles of human serum, aqueous humor and vitreous humor. Metabolomics 16(7):80. https://doi.org/10.1007/s11306-020-01700-3

36. Musshoff F, Klotzbach H, Block W, Traeber F, Schild H, Madea B (2011) Comparison of post-mortem metabolic changes in sheep brain tissue in isolated heads and whole animals using ^{1}H-MR spectroscopy--preliminary results. Int J Legal Med 125(5):741–744. https://doi.org/10.1007/s00414-010-0463-3

37. Michaelis T, Helms G, Frahm J (1996) Metabolic alterations in brain autopsies: proton NMR identification of free glycerol. NMR Biomed 9(3):121–124. https://doi.org/10.1002/(SICI)1099-1492(199605)9:3%3C121::AID-NBM409%3E3.0.CO;2-F

38. Go A, Shim G, Park J, Hwang J, Nam M, Jeong H, Chung H (2019) Analysis of hypoxanthine and lactic acid levels in vitreous humor for the estimation of post-mortem interval (PMI) using LC-MS/MS. Forensic Sci Int 299:135–141. https://doi.org/10.1016/j.forsciint.2019.03.024

39. Donaldson AE, Lamont IL (2013) Biochemistry changes that occur after death: potential markers for determining post-mortem interval. PLoS One 8(11):e82011. https://doi.org/10.1371/journal.pone.0082011

40. Da Cunha EC, Ordóñez-Mayán L, Vázquez MLR, Vieira DN, Febrero-Bande M, Barús JIM (2022) The biochemistry of the vitreous humour in estimating the post-mortem interval-a review of the literature, and use in forensic practice in Galicia (northwestern Spain). Forensic Sci Med Pathol. https://doi.org/10.1007/s12024-022-00539-5